HHS Public Access

Author manuscript

Nat Neurosci. Author manuscript; available in PMC 2012 August 01.

Published in final edited form as:

Nat Neurosci. ; 15(2): 298–307. doi:10.1038/nn.3007.

Visual Map Development Depends On The Temporal Pattern of Binocular Activity in Mice

Jiayi Zhang[1], **James Ackman**[1], **Hong-Ping Xu**[1], and **Michael C. Crair**[1,2,§]

[1]Department of Neurobiology, Yale University, New Haven CT 06510

[2]Department of Ophthalmology & Visual Sciences, Yale University, New Haven CT 06510

Abstract

Binocular competition is thought to drive eye-specific segregation in the developing visual system, potentially through Hebbian synaptic learning rules that are sensitive to correlations in afferent activity. Altering retinal activity can disrupt eye-specific segregation, but little is known about the temporal features of binocular activity that modulate visual map development. We used optogenetic techniques to directly manipulate retinal activity *in vivo* and identified a critical period before eye opening in mice when specific binocular features of retinal activity drive visual map development. Synchronous activation of both eyes disrupted segregation, whereas asynchronous stimulation enhanced segregation. The optogenetic stimulus applied was spatially homogenous, and accordingly retinotopy of ipsilateral projections was dramatically perturbed, but contralateral retinotopy was unaffected or even improved. These results provide direct evidence that the synchrony and precise temporal pattern of binocular retinal activity during a critical period in development regulates eye-specific segregation and retinotopy in the developing visual system.

Keywords

Retinal Waves; Superior Colliculus; Visual Development; Retinotopy; Eye Segregation; Lateral Geniculate Nucleus; Critical Period

INTRODUCTION

Retinal ganglion cell (RGC) projections to the brain form stereotypic maps for eye of origin and retinotopic location, making them an ideal model system to study the development and plasticity of precisely patterned neural circuits[1, 2]. The initial formation of these visual circuits is thought to be guided by molecular cues[3], while the refinement and maintenance[4–6] of these connections appears to be activity-dependent[7]. Substantial evidence

§Corresponding Author: Michael C. Crair, 333 Cedar St., SHM B301; Yale University School of Medicine; New Haven, CT 06510; michael.crair@yale.edu.

AUTHOR CONTRIBUTIONS

J.Z. and M.C.C. designed the experiments. J.Z. conducted the stimulation experiments and analyzed the anatomical data. J.A. and J.Z. conducted the calcium imaging experiments and analyzed the data. H.-P. X. and J.Z. conducted the multielectrode array experiments and analyzed the data. J.Z. and M.C.C. wrote the manuscript.

supports a general role for activity-dependent binocular competition in retinofugal map development. For instance, a relative increase in the amount of activity in one eye leads to the expansion of that eyes' target territory in the dorsal lateral geniculate nucleus (dLGN)[8, 9], indicating that the more active eye makes and further strengthens target synapses when it is at a competitive advantage.

Hebbian synaptic learning rules that may mediate the activity-dependent development of visual maps have been observed in a variety of retinofugal systems, including spike-timing dependent plasticity at retinotectal synapses in tadpoles *in vivo*[10] and burst-timing dependent plasticity at retinogeniculate[11] and retinocollicular[12] synapses in rodents *in vitro*. These observations suggest that synaptic connections are functionally strengthened when cells are synchronously active and weakened when cells are asynchronously active over time windows that are distinct in different model systems[13].

It has long been postulated that the timing of spontaneous wave-like activity in RGCs[14] is critical for the establishment and maintenance of eye-specific segregation through a Hebb-based synaptic learning rule[11, 13] before the onset of vision. The short duration of retinal waves relative to the interval between waves is thought to asynchronously activate the two eyes, resulting in the refinement of eye-specific domains[15]. Evidence for this timing model for binocular competition is extremely limited, with the only direct experimental support coming from classic cat experiments in which artificially asynchronous stimulation of the optic nerves produced neurons that responded predominantly to only one eye, while stimulation of the optic tract, which synchronously activates RGC afferents from both eyes, caused most cells in visual cortex to become functionally binocular[16]. Similarly, alternating monocular occlusion in cats results in reduced cortical binocularity and disrupted depth discrimination[17]. However, these experiments were restricted to a physiological analysis of binocularity in the cortex and manipulated RGC activity after the onset of normal visual experience, when eye segregation in the dLGN and visual cortex has already emerged[2, 18]. Since it has been difficult to precisely manipulate neonatal RGC activity in mammals *in vivo*, the role of timing in the initial development of visual maps remains unexplored.

We chronically manipulated retinal activity in mice before the onset of vision over a range of time scales *in vivo* by expressing a light-gated cation channel Channelrhodopsin-2 (ChR2)[19] directly in RGCs using transgenic and viral transfection methods[20, 21]. Light-driven activation of ChR2-expressing RGCs triggered precisely timed postsynaptic calcium signals in the superior colliculus, demonstrating that optogenetic techniques can reliably drive neuronal response even early in visual development. When the two eyes were synchronously stimulated, we found that the initial emergence of eye-specific domains was disrupted, while asynchronous stimulation improved segregation. After eye-specific domains were already established in the superior colliculus and dLGN, asynchronous stimulation had no effect, but synchronous stimulation caused domains to desegregate. The disruptive effect of optogenetic stimulation on eye segregation waned as the time difference between stimulation of the eyes increased beyond 100 ms, which suggests a sub-second time window for binocular competition. Interestingly, when synchronous stimulation disrupted eye-specific segregation, retinotopy was also dramatically perturbed, but only for ipsilateral RGCs. Both synchronous and asynchronous stimulation slightly improved the retinotopy of

contralateral axons. Finally, all of these effects were limited to a critical period in development that ends around the time of eye-opening. These results demonstrate the importance of precise temporal synchrony of binocular RGC activity in the anatomical development and maintenance of visual maps.

RESULTS

Precise control of RGC neuronal activity

RGCs in mice younger than Postnatal day 10 (P10) do not respond to light through the conventional rod or cone driven pathway[22]. Intrinsically photosensitive RGCs (ipRGCs) have a slow and sluggish response to light from birth, but constitute only a small overall fraction of RGCs[23]. In order to exogenously and precisely manipulate retinal activity in neonatal mice, we first utilized a *Thy1*-ChR2-eYFP (*Thy1*-ChR2) transgenic mouse line that has RGC-specific expression of ChR2[21, 24]. ChR2 in these mice is expressed in a heterogeneous population of RGCs distributed uniformly across the entire retina[24] starting at around P8 (Fig. 1A). ChR2-eYFP expressing RGCs constituted 25.4 ± 3.5% of all the brn3b positive RGCs at P9 (n = 8). Since brn3b labels ~80% of all RGCs[25], ~20% of RGCs expressed ChR2-eYFP in *Thy1*-ChR2 mice at P9. *In vitro* whole cell recording showed that YFP-positive RGCs exhibited sustained spiking activity in response to 470 nm light stimuli with a range of intensities above 0.1625 mW/mm^2 (Fig. 1B). Multielectrode array (MEA) recordings revealed that spike rates were similar for 1 s and 200 ms stimuli (6.4 ± 0.2 Hz for 1 s (n = 70 cells) and 4.7 ± 0.3 Hz for 200 ms (n = 57 cells) at 0.51 mW/mm^2; Fig. 1C-D), which indicates that the number of light-triggered spikes was roughly proportional to the duration of the stimuli. The fraction of all spontaneously active RGCs that were light-responsive was also similar across a wide range of stimulus durations (68.6 ± 5.5%, 55.8 ± 1.4% and 74.4 ± 7.4% for 1s, 200 ms and 5 ms stimuli respectively; Fig. 1D). The light-driven activity was not dependent on synaptic input (Supplementary Fig.1A), confirming it came directly from ChR2 expressing RGCs. We occasionally observed tonic firing that lasted much longer than the duration of the stimuli (Supplementary Fig. 1B); these were likely responses from ipRGCs[23, 26] and were excluded from the analysis. Finally, multiunit recordings showed that the 470 nm light stimuli applied outside the eye could drive neuronal response in the superior colliculus *in vivo* with high temporal precision (Fig. 1E-F). These results confirmed that optogenetic techniques can be used to manipulate RGC activity before the onset of normal vision in mice *in vivo*.

Despite the fact that young mice do not respond to light through conventional retinal pathways, synaptic connections between RGCs and neurons in the superior colliculus exist at birth and mature throughout the first two postnatal weeks[12]. In *Thy1*-ChR2 mice, we examined the spatial and temporal response of neurons in the superior colliculus to optogenetic activation of RGCs using light-triggered calcium signals from superior colliculus neurons labeled with OGB1AM *in vivo* at P9-P10 (Fig. 2A-B). Synchronous stimulation of both eyes (1 s duration) triggered calcium signals in both hemispheres of the superior colliculus simultaneously (Fig. 2C–D). About 30% of the Regions-Of-Interest (ROIs) showed a synchronous increase in fluorescence in response to the synchronous stimulation (Fig. 2E). Response was observed only in the contralateral superior colliculus

when one eye was stimulated, whereas synchronous stimulation of both eyes activated both hemispheres simultaneously (Fig. 2F). The average response frequency for all the ROIs in the contralateral superior colliculus was significantly different from that in ipsilateral superior colliculus ($P = 2 \times 10^{-16}$, Fig. 2G), but similar to the response when both eyes were synchronously stimulated (P = 0.11, Fig. 2G). The minimal ipsilateral response was presumably due to the caudal location of the imaging field; projections from the ipsilateral eye are limited to rostral colliculus, which is obscured by the cortex at this age. This data demonstrates that stimulation of RGCs and the activation of neurons in the superior colliculus can be independently manipulated in each eye using optogenetic strategies in *Thy1*-ChR2 mice *in vivo* early in development.

Timing of binocular activity affects -segregation

RGC axons in mice normally form eye-specific domains in both the superior colliculus and dLGN[27]. At birth, axons from the two eyes are intermingled[27], but axons from the contralateral eye come to occupy exclusively the superficial stratum griseum superficial (SGS) layer of the superior colliculus while ipsilateral axons form domains slightly deeper to the SGS in the stratum opticum layer (SO)[27, 28]. This eye-specific segregation was complete by P9 and remained unchanged thereafter (P = 0.998; Fig. 3). To examine whether binocular activity affected the maintenance of segregation, RGCs from the two eyes were activated synchronously or asynchronously starting at P9 in *Thy1*-ChR2 mice on a 12 hr-cycle for 2–3 days. Precisely synchronous optical stimulation (0.1 Hz, 2.5 s stimuli) caused ipsilateral axons to form multiple aberrant clusters that overlapped with contralateral axons in the SGS (P = 0.0000768; Fig. 3A-B, Supplementary Fig. 2A). Thus, synchronous activation of both eyes caused a desegregation of RGC afferents that were previously segregated. However, asynchronous stimulation (0.1 Hz, 2.5 s stimuli with 5 s asynchrony between two eyes) had no effect on eye-specific segregation (P = 0.431; Fig. 3B), unlike synchronous stimulation (P = 0.00114; Fig. 3B). To further examine whether the effect of synchronous stimulation on eye-specific segregation was directly related to the temporal overlap of RGC activity, we applied synchronous stimuli of varying durations (1 s, 2 s and 2.5 s) at 0.2 Hz. The disruption in eye-specific segregation increased with the duration that stimuli overlapped between the two eyes (one-way ANOVA, $F = 8.87 > F_{0.05}$ (= 3.25), $P < 0.0001$; Fig. 3C). These results show that the maintenance of eye-specific segregation is specifically sensitive to the relative timing and overlap of activity between the two eyes, with synchronous stimulation disrupting eye-specific segregation, while asynchronous stimulation, which has the same overall level of activity, had no effect on segregation.

Interestingly, synchronous stimulation starting at P14 had no effect on eye segregation (P = 0.999; Fig. 3B), demonstrating a critical period for eye-specific segregation in the superior colliculus that ends around the time of eye-opening. Chronic stimulation of one eye starting at P9 disrupted eye-specific segregation in the ipsilateral superior colliculus (P = 0.0299; Fig. 3B), which demonstrates that eye-specific segregation is sensitive to both the overall level and the relative timing of retinal activity, and is similar to the effect of monocular cAMP injections, which elevates RGC activity levels in the treated eye and expands dLGN domains from the active eye[9]. Eye segregation in synchronously stimulated wild type C57 (WT) mice was unaffected (P = 0.957; Fig. 3B), confirming that the segregation phenotype

observed in synchronous stimulated *Thy1*-ChR2 mice was due to the light-triggered activity in ChR2 expressing RGCs.

Timing differences up to 100 ms disturbs segregation

The functional development of retinotectal synapses in *Xenopus laevis* is sensitive to millisecond timing differences in afferent activity[10], and alternating monocular occlusion for durations of 500 ms or longer in cats disrupts the development of functional binocularity in visual cortex[17]. However, the temporal precision of binocular competition in shaping the development of eye-specific segregation is unexplored. In RGCs of *Thy1*–ChR2 mice examined *in vitro*, single spikes were triggered by 5 ms optical stimuli (Fig. 1D). Using trains of these short light pulses (five consecutive 5 ms light pulses with intervals of 400 ms every 5 s; Fig. 4A), we examined the temporal precision of binocular competition. The latencies of single spikes to the stimuli were small and consistent at the light intensity used under *in vivo* conditions (8.8 ± 1.6 ms, Fig. 4B). Precisely synchronous stimulus bursts (time difference 0 s) delivered to each eye disrupted segregation ($P = 0.0163$; Fig. 4A, *C*) in a manner similar to that observed using synchronous stimuli of long duration (Fig. 3). To our surprise, stimulus bursts with only 200 ms offset between each 5 ms stimulus delivered to each eye had no effect on eye-specific segregation ($P = 0.967$; Fig. 4A, *C*). As the temporal difference between each eye's stimulus decreased from 100 ms to 20 ms, eye-specific segregation became progressively more disturbed ($P = 0.170$ for 100 ms, $P = 0.0182$ for 50 ms and $P = 0.01224$ for 20 ms in comparison to Ctrl; One-way ANOVA, $F = 4.366 > F_{0.05}$ (= 3.06), $P < 0.01$; Fig. 4A, *C*) and the number of ipsilateral axon clusters mislocalized in the contralateral SGS layer increased accordingly (Fig. 4D). This suggests that binocular competition driving eye-specific segregation depends on timing differences in RGC activity between the two eyes of about 100 ms. This is shorter than the second-long timing difference predicted based on the dynamics of spontaneous retinal waves[11, 29], but much longer than the 5–10 ms time window observed at retinotectal synapses in frogs[10].

Early asynchronous stimulation improves segregation

In *Thy1*-ChR2 mice, synchronous stimulation of the two eyes disrupted eye-specific segregation during the second week after birth (Fig. 3). However, segregation of retinofugal projections in mice emerges in the first week after birth (Supplementary Fig. 3), when ChR2 expression is still weak in *Thy1*-ChR2 mice. To overcome this limitation and examine the role of RGC activity timing and binocular competition in the initial development of eye-specific segregation, we injected AAV-DIO-ChR2-mCherry virus into the ventral-temporal (binocular) retina of Rx-CRE mice at P0-P1 and began optical stimulation at around P5. At this age, eye-segregation is just emerging (Supplementary Fig. 3), but ChR2 expression was robust (Fig. 5A) and RGC response to optical stimulation was similar to *Thy1*-ChR2 mice at P9 (Average firing rate is 4.4 ± 0.6 Hz (n = 34 cells), fraction of light–responsive channels among all active channels is 44.9 ± 4.5% (n = 6); Fig. 5B). Synchronous stimulation (0.2 Hz, 1.5 s) of both eyes between P5 and P7 disrupted eye–specific segregation ($P = 0.0000254$; Fig. 5C), as it did in the second week after birth in *Thy1*-ChR2 mice. However, unlike similar experiments conducted in the second week, asynchronous stimulation (0.2 Hz, 1.5 s, 2.5 s difference between two eyes) between P5 and P7 improved eye-specific segregation in comparison to unstimulated control mice ($P = 0.015$, Fig. 5C), suggesting that

the additional asynchronous activity produced by optogenetic stimulation actually improves eye-specific segregation. These results argue strongly that the relative timing of ongoing activity in the two eyes mediates both the initial segregation and the maintenance of eye-specific retinofugal projections in mice during the first two weeks after birth.

Asynchronous stimulation rescues -segregation in $\beta2^{-/-}$ mice

Mice lacking the $\beta2$ subunit of nicotinic acetylcholine receptors ($\beta2^{-/-}$) have abnormal first week cholinergic retinal waves and disrupted eye-specific segregation in both the superior colliculus and LGN[28, 30, 31]. Eye–specific segregation partially recovers in $\beta2^{-/-}$ mice during the second week after birth through the activity of glutamatergic retinal waves[30, 31]. We crossed *Thy1*-ChR2 mice to $\beta2^{-/-}$ mice (ChR2;$\beta2^{-/-}$) to further examine the role of asynchronous retinal activity on eye-specific segregation. Synchronous stimulation starting at P9 in ChR2;$\beta2^{-/-}$ mice further degraded eye-specific segregation (Fig. 6A; P = 0.000255), like in *Thy1*-ChR2 (Fig. 2B) and ChR2;$\beta2^{+/-}$ mice (Fig. 6B; P = 0.00757). However, asynchronous stimulation of ChR2;$\beta2^{-/-}$ mice actually improved segregation in comparison to unstimulated ChR2;$\beta2^{-/-}$ controls (P = 0.00286; Fig. 6A), unlike in *Thy1*-ChR2 (Fig. 2B) and ChR2;$\beta2^{+/-}$ mice (Fig. 6B; P = 0.9969), where asynchronous stimulation had no effect on segregation. These results show that in $\beta2^{-/-}$ mice, asynchronous stimulation dramatically improved eye segregation, whereas the modest segregation that does exist in $\beta2^{-/-}$ mice was worsened by synchronously stimulating the two eyes. In summary, synchronous stimulation during the first two weeks after birth disrupted eye-specific segregation regardless of the initial segregation status; asynchronous stimulation improved immature or impaired segregation, but did not affect segregation that was already established.

Synchronous stimulation disrupts segregation in the dLGN

The effects of optogenetically induced binocular activity on eye-specific segregation in the dLGN were similar to but smaller than those observed in the superior colliculus (Fig. 7A-B). In comparison to unstimulated controls, synchronous binocular stimulation starting at P9 in *Thy1*-ChR2 mice increased the overlap between ipsilateral and contralateral eye afferents in the dLGN (P = 0.042; Fig. 7A) as well as the fraction of the dLGN covered by ipsilateral projections (P = 0.0115; Fig. 7A). The fraction of the dLGN covered by contralateral projections did not change (0.901 ± 0.013 for Ctrl, 0.879 ± 0.021 for Sync, and 0.871 ± 0.018 for Async; P > 0.05 for all comparisons). In ChR2;$\beta2^{-/-}$ mice, synchronous stimulation also increased the fraction of the dLGN covered by ipsilateral RGC afferents (P = 0.0066; Fig. 7B) and appeared to cause a similar increase in the overlap between ipsilateral and contralateral projections, but this latter difference did not reach statistical significance (P = 0.088; Fig. 7B). The fraction of the dLGN covered by contralateral projections in optogenetically stimulated ChR2;$\beta2^{-/-}$ mice did not change (0.873 ± 0.008 for Ctrl, 0.851 ± 0.011 for Sync, and 0.879 ± 0.006 for Async; P > 0.05 for all comparisons). In summary, synchronous optogenetic stimulation had similar but smaller effects on eye-specific segregation in the dLGN as the superior colliculus, causing expansion of the ipsilateral eye projection without significant effects on the contralateral eye projection.

Effects of optogenetic stimulation on retinotopy

In addition to molecular cues, we and others have argued that the spatiotemporal pattern of spontaneous retinal waves is important in the development of both eye-specific segregation and the refinement of retinotopy[7, 9, 32, 33]. This argument hinges on the spatially restricted nature of propagating retinal waves in which the activity of neighboring RGCs is much more correlated than distant RGCs, providing an instructive signal for retinotopic refinement. We tested this hypothesis by examining the effect of optogentic stimulation on retinotopic refinement. The optical stimulus we applied is spatially uniform, producing synchronous firing across the entire array of ChR2 expressing RGCs (Fig. 1D and Fig. 2C). For this analysis, we first examined the position of ipsilateral axon clusters in the superior colliculus of optogenetically stimulated and control *Thy1*-ChR2 mice (Fig. 8A). Ipsilateral axons from the ventral–temporal retina projecting to the contralateral SGS layer were often mislocalized in mice that were synchronously stimulated, with many axon clusters abnormally terminating in the caudal superior colliculus, which normally contains projections from dorsal-nasal retina (Fig. 8A). Control (unstimulated) and asynchronously stimulated mice retained only their appropriate anatomical projections to the rostral portion of the SO layer of the superior colliculus just below the SGS (Fig. 8A). This confirms that uniform retinal stimulation can dramatically disrupt retinotopy, but the effect was limited to ipsilateral axons that mis-segregated in the contralateral SGS layer. Contrary to our expectation, optogenetic stimulation in *Thy1*-ChR2 mice caused dorsal RGCs, which project only to the contralateral superior colliculus, to form *smaller* target zones in the superior colliculus than unstimulated *Thy1*-ChR2 control mice ($P = 0.03104$; Fig. 8B, *D*), regardless of whether the two eyes were stimulated synchronously or asynchronously ($P = 0.2396$, data not shown). These smaller target zones suggest greater retinotopic refinement of RGC projections to the superior colliculus. RGCs from the ventral-temporal retina, which project bilaterally in mice, also appeared to have slightly *smaller* target zones in the contralateral superior colliculus after stimulation relative to unstimulated *Thy1*-ChR2 control mice, but the trend was not statistically significant ($P = 0.09283$; Fig. 8C, *D*). In ChR2;$\beta2^{-/-}$ mice, which have large and unrefined target zones to begin with, both dorsal and ventral-temporal RGCs also formed much *smaller* target zones in stimulated animals than in unstimulated ChR2;$\beta2^{-/-}$ control mice (Dorsal $P = 0.03724$; Ventral-temporal $P = 0.0002644$; Fig. 8E-G), regardless of whether the two eyes were stimulated synchronously or asynchronously (Dorsal $P = 0.1353$, Ventral-temporal $P = 0.1262$, data not shown). These results demonstrate that uniform retinal stimulation during development can dramatically disrupt retinotopy, but these retinotopic effects were limited to ipsilateral axons that were mis-segregated in the SGS. In contrast, the effect of uniform retinal stimulation on retinotopy of contralateral axons was more modest, and retinotopy was improved both for asynchronously and synchronously stimulated retinas, perhaps due to the increased retinal activity provided by exogenous optogenetic stimulation.

DISCUSSION

Rhythmic spontaneous activity exists in many developing neural circuits, including the cochlea[34], cortex[35], cerebellum[36] and spinal cord[37]. Perhaps nowhere else in the nervous system has this spontaneous activity been examined more closely than the developing visual

system[7], which continues to serve as a touchstone for understanding the role of neuronal activity in the formation and functional organization of neural circuits throughout the brain. By optogenetically manipulating the temporal pattern of retinal afferent activity in both eyes *in vivo*, here we demonstrated that the level and precise timing of binocular activity markedly influence the development of neural circuits even before the onset of vision. Neural circuit development may be generally sensitive to the timing of spontaneous neural activity, particularly in bilateral sensory systems[37].

The striking contrast in the effects of synchronous and asynchronous stimulation on eye–specific segregation, despite these paradigms differing only in the relative timing of the stimulus presented to the two eyes, directly implicates a Hebb-based activity-dependent competitive process in the initial emergence of eye-specific segregation. Previous similar attempts to examine the role of timing in visual map development were restricted to a physiological analysis that manipulated RGC timing (and activity levels) *after* maps already formed[2, 16, 18]. Here, we've shown that the initial development of eye-specific domains is enhanced or degraded based solely on the relative timing of binocular activity, which directly demonstrates that visual map development is sensitive to a mechanism that compares the temporal pattern of ongoing activity in the two eyes.

Temporal features of RGC activity that promote segregation

In the developing visual system of fish and frogs, millisecond timing differences in RGC afferent activity produces spike-timing dependent plasticity at retinotectal synapses that reliably alters the receptive field properties of neurons in the optic tectum[10, 38]. These lower vertebrates lack spontaneous activity in the developing retina but are visually responsive as soon as RGC axons reach the tectum, indeed they rely on vision to locate food and evade predators long before their visual systems are mature[39]. In contrast, *in vitro* studies of synaptic learning rules at retinofugal synapses[11, 12] and analysis of the spatiotemporal properties of retinal waves[14, 29] suggest that the relevant time scale for activity-dependent development of visual maps in mammals is on the order of seconds, rather than milliseconds. By manipulating the temporal pattern of RGC activity and determining the effect on eye-specific segregation, we were able to directly examine the temporal rules that govern eye-specific segregation *in vivo*. These experiments showed that the disruption caused by synchronous stimulation on eye-specific segregation is proportional to the overlap in activity between the eyes, but stimuli that were separated by as much as 100 ms still impaired segregation. Moreover, synchronous, single 5 ms pulses at 0.2 Hz had no effect on eye-specific segregation, but bursts of synchronous 5 ms pulses at the same frequency disrupted segregation (Supplementary Fig. 4). This suggests that bursting of RGCs on a ~100 ms time scale, rather than the timing of individual spikes, instructs the development of visual maps in mammals[12, 29, 40], and is consistent with the features of retinal waves recorded *in vitro*[14, 29]. Spike-timing dependent plasticity is thought to be regulated by the dynamics of Ca^{2+} influx through N-methyl-D-aspartate Receptors (NMDARs) and further modulated by slower biochemical processes within the cell[41]. The burst-timing dependent plasticity described here is probably mediated by similar mechanisms, as the ~100 ms time scale is consistent with neuronal membrane and receptor kinetics, but is likely too short to be directly mediated by biochemical processes.

The temporal pattern of spontaneous RGC activity may also be informative for other aspects of visual system development. During the second week after birth, ON and OFF RGCs in the same eye have precisely timed asynchronous spontaneous activity that is thought to refine connections of functionally distinct (ON/OFF) circuits in mice[40]. In the ferret, exogenous synchronous optic nerve stimulation of one eye disrupts the development of orientation selectivity in the visual cortex[42]. It's possible that spatiotemporal patterns of spontaneous RGC activity were acquired over evolutionary development to harness the same cellular and synaptic mechanisms that mediate map development through visual experience in lower vertebrates and experience-dependent visual system plasticity later in life in mammals.

Critical period plasticity affects ipsilateral projections

Stimulus induced plasticity of eye-specific projections during a critical period in development has not previously been reported in the superior colliculus, but similar effects are well known in the dLGN and visual cortex[7]. Interfering with ongoing spontaneous retinal waves also induces the desegregation of retinal afferents to the dLGN[4–7, 43]. We observed that ipsilateral axons that mis-segregate into the contralateral superior colliculus due to synchronous optogenetic stimulation form local, clustered mis-projections. This is in clear contrast to the segregation phenotypes observed in $\beta2^{-/-}$ mice and other retinal wave mutant mice, which have ipsilateral axon arbors that are diffusely spread across the SGS layer[28, 31, 44]. One explanation for this difference is the sparseness of ChR2-expressing RGCs in our optogenetic manipulation. The available evidence suggests that a heterogeneous population of RGCs express ChR2 in our manipulation[24], so it is also possible that the optogenetic stimulation impaired segregation only in distinct subclasses of these RGCs[45], leading to local clusters of axon arbors in the wrong layer instead of diffuse misprojections from a large cohort of different RGC classes in $\beta2^{-/-}$ mice. Alternatively, the cellular mechanism causing the diffuse segregation phenotype in $\beta2^{-/-}$ mice may be distinct from that observed here, perhaps because it is sensitive mainly to the significantly reduced overall levels of activity in these mutants.

Interestingly, optogenetic stimulation had no apparent effect on eye-segregation of contralateral RGC projections (no overgrowth into the ipsilateral domain) regardless of whether the stimulus was synchronous or asynchronous between the eyes. Ipsilateral axons may be more susceptible to the effects of a binocular competitive process than contralateral axons[46], possibly because of their molecularly distinct properties[47] or because their development is delayed relative to contralateral projections[48]. As a result, stimulus-dependent effects on contralateral axon segregation may be absent, subtle, or require more sustained periods of altered activity before they become apparent in our assays.

Eye segregation defects in the dLGN

Synchronous bilateral optogenetic stimulation produced eye segregation defects in the dLGN as well as the superior colliculus, suggesting that the development of eye-specific segregation is governed by similar activity-dependent processes in the dLGN and superior colliculus. However, the effects of synchronous stimulation in the dLGN were smaller than in the superior colliculus, and asynchronous stimuli that improved eye segregation in the

superior colliculus had limited effect in the dLGN. This may be related to intrinsic differences in the development and structure of RGC axon arbors in the dLGN and SC[44]. Another cause for this difference may be the sizable population of ipRGCs that respond to blue light[23] and project to the dLGN[26]. IpRGC projections to the superior colliculus are more sparse than the dLGN[26], and we did not observe ipRGC responses in the superior colliculus in electrophysiological and optical imaging experiments *in vivo* (data not shown), though we did occasionally encounter RGC responses in our MEA recordings *in vitro* that were reminiscent of ipRGCs (Supplementary Fig. 1B). In addition, no rod- or cone-mediated signaling to RGCs is present in pups younger than P9[22], and eye-specific segregation for synchronously stimulated wild-type animals was normal (Fig. 3B). This indicates that activity in the superior colliculus triggered by optogenetic stimuli derived mainly from RGCs expressing ChR2, and ipRGCs did not play a major role in the visual map phenotypes in the superior colliculus, but the sustained firing properties of ipRGCs may have weakened the effect of asynchronous stimuli on eye segregation in the dLGN.

RGC activity in retinotopic map refinement

Like eye–specific segregation, the development of retinotopic maps may be governed by both molecular factors and neuronal activity[30, 32]. In particular, the highly correlated firing of neighboring but not distant RGCs during spontaneous retinal waves is thought to drive retinotopic map refinement[7, 28]. Unlike retinal waves, the light stimulus we used was homogeneous and lacked spatial cues that could be used to encourage retinotopic refinement. Accordingly, we observed that optogenetic stimulation dramatically perturbed retinotopy in mis-segregated, synchronously stimulated ipsilateral axons; many of these ipsilateral axon arbors from ventral-temporal retina terminated in caudal portions of the superior colliculus that normally represent lateral or dorsal-lateral positions in the contralateral retina. A link between eye-specific segregation and retinotopy is consistent with recent reports of ‘yoked’ effects between segregation and retinotopy in mice with spatially restricted ‘small’ retinal waves[28] and in ferrets with disrupted ocular dominance columns due to early retinal activity blockade[49]. Surprisingly, the retinotopy of ipsilateral axons in asynchronously stimulated mice was unperturbed, and optogenetic stimulation had no effect or even *improved* retinotopic refinement of contralateral axons, regardless of whether the stimulation was synchronous or asynchronous. These results imply that retinotopic refinement may be more sensitive to the presence and frequency of bursting RGC activity, rather than the spatial pattern of that activity. Alternatively, the sparse distribution of ChR2-expressing RGCs (only 1 in 4 RGCs express ChR2 on average in *Thy1*-ChR2 mice, Fig. 1A-) may produce a spatially inhomogeneous retinal response that is sufficient to drive retinotopic refinement despite the homogeneity of the optical stimulus. Future experiments that enable the synchronous activation of all RGCs (and not just a subset as presented here) may verify whether correlated activity of neighboring RGCs affects the refinement of retinotopy.

In summary, our results demonstrate that the level and precise temporal pattern of binocular retinal activity regulates visual map development even before the onset of vision in mice. This is consistent with a Hebb-based synaptic plasticity rule that directly links the timing of activity between pre- and post-synaptic neurons with changes in neuronal and circuit

morphology and function. Of course, our data does not exclude the possibility that an unknown molecular process regulated by the temporal pattern of *binocular* neuronal activity and independent of Hebb-based plasticity at the synapse drives visual map development. Whatever the case, the mechanism driving visual map development is sensitive to 100 ms timing differences in neuronal activity between the eyes.

METHODS

Animals and virus

Animals were treated in compliance with the Yale IACUC, U. S. Department of Health and Human Services and Institution guidelines. Wild type (WT) mice (C57BL/6J) and *Thy1*-ChR2–eYFP (*Thy1*-ChR2) mice (line 18) were obtained from The Jackson Laboratory (Stock Number: 007612). *Thy1*-ChR2 mice were genotyped following the protocol from The Jackson Laboratory. ChR2; $\beta 2^{-/-}$ mice were generated by crossing *Thy1*-ChR2–EYFP mice with $\beta 2^{-/-}$ mice[30],. Both *Thy1*-ChR2 and ChR2; $\beta 2^{-/-}$ were maintained on a C57bl/6 background. Rx-CRE transgenic mice [50] were maintained on a mixed background and genotyped by genomic PCR using primer sequences previously described [50]. rAAV5/EF1α-DIO(Doublefloxed Inverse Orf)-ChR2-mCherry (AAV-DIO-ChR2-mCherry) virus (10^{11}~10^{12} viral molecules/mL) was obtained from the Vector Core Facility at the University of North Carolina. *n* represents the number of animals in the manuscript unless otherwise specified.

Electrophysiology

Whole cell light responses were recorded in a standard patch clamp rig. The retina was dissected in Ringer's solution containing (in mM): NaCl 124, KCl 2.5, $CaCl_2$ 2, $MgCl_2$ 2, NaH_2PO_4 1.25, $NaHCO_3$ 26, and glucose 22 (pH 7.35 and oxygenated with 95% O_2 and 5% CO_2) and mounted under a fluorescence dissection microscope. A pulled glass pipette (~5–8 MΩ) filled with internal solution (containing (in mM): K-Gluconate 105, KCl 5, $CaCl_2$ 0.5, $MgCl_2$ 2, 5 ethylene glycol-bis(2-aminoethylether)-N,N,N0,N0-tetraacetic acid (EGTA) 5, HEPES 10, ATP-Mg 4, GTP-Na 0.5, Phosphoreatine-Na 7, pH 7.4) patched onto a YFP fluorescent ganglion cell; stimulation light from the mercury lamp (max 35 mW/mm^2, FITC excitation filter 480/40 nm) was provided through the 40X water-immersion objective.

Multi-channel RGC responses were recorded using a multielectrode array (60 channels, 100 μm apart; Multichannel systems) at 37°C in Ringer's solution (same as the whole cell recording conditions). Stimulating light was provided from the back of the recording chamber using a blue LED (Luxeon K2 blue, Philips), whose intensity and timing were controlled by a square pulse generator (S88X, Grass Technologies). Action potentials were thresholded offline (40 μV) and filtered between 100 Hz and 3 kHz. Offline data were analyzed using Offline Sorter (Plexon), Neuro Explorer (Nex Technologies) and a custom program.

In vivo calcium imaging and extracellular recording

Thy1-ChR2 mice aged P9-P10 were deeply anesthetized with isoflurane (2.5%) in oxygen and then placed on a heating pad set to 36.5°C via a homeothermic temperature monitor

(NPI TC-20, ALA Scientific). Local anesthesia was produced by subcutaneous injection (0.05 ml) of 1% Xylocaine (10 mg/ml lidocaine/0.01 mg/ml epinephrine, AstraZeneca) under the scalp. After removal of the scalp, steel head posts were fixed to the exposed skull using cyanoacrylate glue. Isoflurane anesthesia was adjusted between 0.5–1.0% as necessary to maintain a stable respiratory rate. For electrophysiological recordings, an AgCl reference ground wire was placed on the cerebellum through a small burr hole made in the occipital skull. A ~2 mm oval craniotomy was created just posterior to lambda using the tip of an 18G syringe needle. After achieving hemostasis, the dura was carefully removed. The craniotomy was filled with warm (37°C) agarose (A9414, Sigma, 1.5% in sterile buffered saline, 150mM NaCl, 2.5 mM KCl, 10 mM HEPES, pH 7.4).

Extracellular multiunit activity recordings were performed using epoxylite insulated tungsten microelectrodes (0.5–1.0 MΩ, FHC, Inc.) –. Electrodes were lowered into the superior colliculus to a depth of 50–300 μm below the pial surface. Signals were amplified and band-pass filtered at 300 - 5000 Hz (Multichannel Systems MPA8 headstage and A-M Systems Model 3500) and sampled at 25 kHz with a Power 1401 and Spike2 software (Cambridge Electronic Design).

The calcium indicator Oregon Green BAPTA-1-AM (OGB1-AM; Invitrogen) was prepared by dissolving 50 μg of dye in 4 μl 20% pluronic acid in DMSO (Invitrogen) and 35 μl of sterile buffered saline (150 mM NaCl, 2.5 mM KCl, 10 mM HEPES, pH 7.4) and 1 μl of 10 mM Alexa 594 hydrazide (Invitrogen) and sonicating for 20 min. The solution was then filtered through a 0.45 μm microcentrifuge filter (Millipore).

Pulled glass micropipettes (1B150F-4; World Precision Instruments) were loaded with OGB1-AM dye solution, and inserted into an electrode holder connected to a Picospritzer III (10 psi, General Valve Corp). Bulk labeling with OGB1-AM was achieved at 2–4 injection sites per hemisphere, by lowering the pipette to a depth of 100–300 μm below the pial surface of the superior colliculus with a motorized micromanipulator (MP-225, Sutter) and delivering 60 brief (20 msec) pressure pulses. A circular, 5 mm diameter #1.5 coverglass (Warner Instruments) was placed over the craniotomy in fresh agarose and stabilized with Kwik-Sil (World Precision Instruments). The eyelids were cut and glued open; atropine (Neogen Vet) and sunflower seed oil (Sigma) was applied to both eyes to dilate the pupil and prevent the eyeball from drying out. Blue LEDs (bandpass filtered 450 – 490 nm) were used to stimulate both eyes independently with a Square Pulse Stimulator (S88X, Grass Technologies). A 1 hr recovery period in the dark was allowed before the experiment.

A CCD camera (Pixelfly, The COOKE Corporation) coupled to an Olympus BX51 and a 2.5x 0.075NA objective (Zeiss #440310-9903) was used to image calcium responses in both hemispheres of the superior colliculus simultaneously. Epifluorescent illumination was done using an Hg^{2+} light source (X-Cite Series 120, EXFO) through a neutral density filter and a filter cube set (U-MGFPHQ, Olympus) with a CCD exposure of 200 msec.

Image processing was performed using a custom MATLAB program. A rectangular grid of ROIs (for each ROI; h =45 μm, w = 45 μm) was masked over the average image, F_0, of visible OGB1AM fluorescence for each hemisphere of a movie. Calcium signals for each

ROI was the average fluorescence intensity inside each ROI in each frame, F_t, measured as a function of time ($dF/F = (F_t - F_0)/F_0$). Calcium transients were detected using automatic detection routines to identify local maxima (>2 standard deviations of the derivative of the signal). Peri-stimulus time histograms were calculated for every ROI of a movie, using an interval window of [–300, 800 ms] around each stimulus time to find the set of detected calcium transient onsets. The normalized response frequency for each ROI was calculated as the total number of detected calcium onsets divided by the number of stimulus presentations. For each ROI of each hemisphere, the normalized anterior-posterior and medial-lateral distances were calculated as the ROI centroid distance from the most anterior-medial location in the dye labeled craniotomy image normalized to the most posterior and lateral locations in the dye labeled craniotomy image.

In vivo light stimulation

Pups were anesthetized by hypothermia for 1 minute and wrapped in gauze tightly prior to stimulation. The eyelids were cut and glued open; atropine and sunflower seed oil was applied to both eyes to dilate the pupil and prevent the eyeball from drying out. 3 pups at a time were kept in a standard isoflurane chamber (VetEquip) for 12 hours with 0.7% isoflurane. Six blue LEDs were used to stimulate each eye separately of each pup *in vivo*. The light intensity was 0.64 mW/mm^2 immediately outside the cornea of the eye, with the right eye leading the left eye for asynchronous stimuli. Control animals went through the same surgical procedure and were kept in the isoflurane chamber alongside the experimental mice, but were not subject to light stimulation. The timing and duration of each LED light stimulus was controlled by a Master 8 pulse stimulator (A.M.P.I.), triggered by a Square Pulse Stimulator for each cycle of stimulation. After stimulation, the glue was removed from the eyelid and pups were recovered from anaesthesia on a temperature controlled heating pad before returning to the mom.

Virus and dye injections

P0-P1 Rx-CRE pups were anesthetized by hypothermia for 3–4 minutes prior to injection surgery. AAV-DIO-ChR2-mCherry virus was filled into pulled glass pipettes (tip diameter 2~3 μm) and injected intravitreously in the ventral-temporal region (binocular zone) of each eye (350 nL) using the Nanoject II system (Drummond Scientific Company) at its original titer. *Thy1*-ChR2 post-stimulation pups at P11-P12 were anaesthetized with a veterinary anesthetic cocktail (in mg/ml: 4.28 ketamine, 0.82 xylazine and 0.07 acepromazine) at a dosage of 100 μL/g bodyweight. Focal DiI injections (2.3 nl) for measurements of retinotopy were performed as previously described [28, 30]. Briefly, lipophilic dye 1,1′-dioctadecyl-3,3,3′,3′-tetramethylindocarbocyanine perchlorate (DiI, molecular probes) (2.3 nl) was injected into the retina using the Nanoject II system to label a small group of neighboring RGCs. Injections were localized along the perimeter of the retina, using the insertion points of the four major eye muscles as reference [28]. For eye-specific segregation experiments, whole-eye injections were performed as previously described [28]. Briefly, 1.5 μL Alexa fluor-conjugated cholera toxin (Molecular Probes) was injected intravitreously using a pulled glass pipette (tip diameter ~5 μm) (Alexa 488 (green) for the left eye and Alexa 555 (red) for the right eye). Animals were placed on a temperature controlled heat pad after surgery and returned to the mom upon recovery from anesthesia.

Fluorescent image acquisition and analysis

48 h after whole eye injection, animals were sacrificed and transcardially perfused. For eye segregation experiments, brains were dissected, fixed in 4% paraformaldehyde (PFA) overnight and mounted in 3% agarose. 150 μm brain slices were sectioned coronally (dLGN) or sagitally (superior colliculus) using a vibratome (1000VT, Leica). Three slices of dLGN with the largest ipsilateral projection area and four slices of superior colliculus 150 μm lateral to the midline were collected for imaging and analysis. For retinotopy experiments, animals were sacrificed 48 h after DiI injection.

Fluorescent images were acquired using a Zeiss ApoTome microscope and AxioVision Software (Zeiss, Germany). Quantification of eye-specific segregation was conducted blind to experimental conditions. Analysis of all images used a custom Matlab program from previous reports [28]. For the superior colliculus, the territory of axon terminals from the contralateral (green-SGS) eye was outlined based on the green fluorescent signal. The overlap of these (SGS) pixels demonstrating fluorescence from the ipsilateral (red) eye was quantified at different thresholds (Supplementary Fig. 2B). Images with a threshold of 10 were composed of pixels with intensity larger than 10% of the maximum intensity, which were chosen for quantification throughout because it best illustrated the clustering, though the phenotype was consistent across a range of thresholds (Supplementary Fig. 2C). The relative position of the ipsilateral cluster was quantified by determining the value of a/(a+b), where a is the distance from the cluster to the caudal end of the SGS and b is the distance from the cluster to the rostral end of the SGS. For LGN, the overlap (in %) between ipsilateral and contralateral fluorescence pixels was measured at different thresholds. The overlap images were acquired by applying AND to binary ipsilateral and contralateral images in Image J.

Quantification of retinotopy was conducted using a custom Matlab program as described before [28, 30]. Briefly, the superior colliculus was manually outlined and its area was measured. To quantify the DiI labelled target zone, the number of pixels above half-maximum fluorescence intensity was measured. The size of the target zone was calculated by dividing the area of half–maximum target by the total superior colliculus area. As a control, the average sizes of the DiI injection in the retina (measured in AxioVision) were similar for control and experimental groups (Supplementary Fig. 5). The coefficient of determination (R^2) for linear regression in each group was calculated in Origin. An R^2 near 0 indicates that the fit is close to a y = <y> fit. An R^2 near 1 indicates that the fit is close to a linear fit.

Statistical analysis

All statistical analysis was conducted using One-Way ANOVA in Origin. All P values in the text are calculated from pair-wise comparisons with Tukey test unless specified. The Alpha level was 0.05. A Shapiro-Wilk test was conducted to determine normality of the data.

Immunostaining

Retinas of *Thy1*-ChR2 mice were dissected under the same conditions as for brain dissections described above. Whole-mount retinas were permeabilized with 0.5% Triton-

X100 in 1X PBS for 20 mins and blocked with 2% donkey serum and 2 mg/mL BSA in 1X PBS containing 0.05% Triton-X100 overnight at 4 °C. Retinas were then incubated in primary antibody (brn-3b, 1:50, Santa Cruz Biotechnology, Inc) in blocking solution for 2 days at 4 °C followed by six times wash in 1X PBS containing 0.01% Triton-X100. Secondary antibody (Alexa568-donkey-anti-goat, 1:200, Jackson ImmunoResearch Laboratory, Inc) in blocking solution was applied to the retinas for 2 days of incubation at 4 °C. After washing three times in 1X PBS, retinas were mounted with Fluromount-G (Electron Microscopy Science) for imaging. Image J was used to count cell numbers.

Supplementary Material

Refer to Web version on PubMed Central for supplementary material.

Acknowledgments

We would like to thank members of the Crair lab, Jessica Cardin and Mike Higley for valuable comments on the manuscript and Yueyi Zhang for technical help. This work was supported by NIH grants P30 EY000785, R01 EY015788 and R01 EY015788S to MCC, and an RPB Challenge Grant to the Department of Ophthalmology & Visual Sciences. MCC also thanks the family of William Ziegler III for their support.

References

1. Rakic P. Prenatal genesis of connections subserving ocular dominance in the rhesus monkey. Nature. 1976; 261:467–471. [PubMed: 819835]
2. Shatz CJ. The prenatal development of the cat's retinogeniculate pathway. The Journal of Neuroscience. 1983; 3:482–499. [PubMed: 6402566]
3. Feldheim DA, O'Leary DD. Visual map development: bidirectional signaling, bifunctional guidance molecules, and competition. Cold Spring Harb Perspect Biol. 2010; 2(11):a001768. [PubMed: 20880989]
4. Chapman B. Necessity for Afferent Activity to Maintain Eye-Specific Segregation in Ferret Lateral Geniculate Nucleus. Science. 2000; 287:2479–2482. [PubMed: 10741966]
5. Demas J, et al. Failure to Maintain Eye-Specific Segregation in nob, a Mutant with Abnormally Patterned Retinal Activity. Neuron. 2006; 50:247–259. [PubMed: 16630836]
6. Koch SM, et al. Pathway-Specific Genetic Attenuation of Glutamate Release Alters Select Features of Competition-Based Visual Circuit Refinement. Neuron. 2011; 71:235–242. [PubMed: 21791283]
7. Huberman AD, Feller MB, Chapman B. Mechanisms Underlying Development of Visual Maps and Receptive Fields. Annual Review of Neuroscience. 2008; 31:479–509.
8. Hayakawa I, Kawasaki H. Rearrangement of Retinogeniculate Projection Patterns after Eye-Specific Segregation in Mice. PLoS ONE. 2010; 5:e11001. [PubMed: 20544023]
9. Stellwagen D, Shatz CJ. An Instructive Role for Retinal Waves inthe Development of Retinogeniculate Connectivity. Neuron. 2002; 33:357–367. [PubMed: 11832224]
10. Mu Y, Poo M-m. Spike Timing-Dependent LTP/LTD Mediates Visual Experience-Dependent Plasticity in a Developing Retinotectal System. Neuron. 2006; 50:115–125. [PubMed: 16600860]
11. Butts DA, Kanold PO, Shatz CJ. A Burst-Based "Hebbian" Learning Rule at Retinogeniculate Synapses Links Retinal Waves to Activity-Dependent Refinement. PLoS Biol. 2007; 5:e61. [PubMed: 17341130]
12. Shah RD, Crair MC. Retinocollicular Synapse Maturation and Plasticity Are Regulated by Correlated Retinal Waves. The Journal of Neuroscience. 2008; 28:292–303. [PubMed: 18171946]
13. Butts DA, Kanold PO. The applicability of spike time dependent plasticity to development. Frontiers in Synaptic Neuroscience. 2010; 2
14. Meister M, Wong RO, Baylor DA, Shatz CJ. Synchronous bursts of action potentials in ganglion cells of the developing mammalian retina. Science. 1991; 252:939–943. [PubMed: 2035024]

15. Moody WJ, Bosma MM. Ion Channel Development, Spontaneous Activity, and Activity-Dependent Development in Nerve and Muscle Cells. Physiological Reviews. 2005; 85:883–941. [PubMed: 15987798]
16. Stryker MP, Strickland SL. Physiological segregation of ocular dominance columns depends on the pattern of afferent electrical activity. Investigative Ophthalmology and Visual Science. 1984; 25(Suppl):278. [PubMed: 6321388]
17. Altmann L, Luhmann HJ, Greuel JM, Singer W. Functional and neuronal binocularity in kittens raised with rapidly alternating monocular occlusion. Journal of Neurophysiology. 1987; 58:965–980. [PubMed: 3694253]
18. Crair MC, Horton JC, Antonini A, Stryker MP. Emergence of ocular dominance columns in cat visual cortex by 2 weeks of age. The Journal of Comparative Neurology. 2001; 430:235–249. [PubMed: 11135259]
19. Boyden ES, Zhang F, Bamberg E, Nagel G, Deisseroth K. Millisecond-timescale, genetically targeted optical control of neural activity. Nat Neurosci. 2005; 8:1263–1268. [PubMed: 16116447]
20. Cardin JA, et al. Targeted optogenetic stimulation and recording of neurons in vivo using cell-type-specific expression of Channelrhodopsin-2. Nat Protocols. 2010; 5:247–254. [PubMed: 20134425]
21. Wang H, et al. High-speed mapping of synaptic connectivity using photostimulation in Channelrhodopsin-2 transgenic mice. Proceedings of the National Academy of Sciences. 2007; 104:8143–8148.
22. Johnson J, et al. Melanopsin-dependent light avoidance in neonatal mice. Proceedings of the National Academy of Sciences. 2010; 107:17374–17378.
23. Berson DM, Dunn FA, Takao M. Phototransduction by Retinal Ganglion Cells That Set the Circadian Clock. Science. 2002; 295:1070–1073. [PubMed: 11834835]
24. Thyagarajan S, et al. Visual Function in Mice with Photoreceptor Degeneration and Transgenic Expression of Channelrhodopsin 2 in Ganglion Cells. The Journal of Neuroscience. 2010; 30:8745–8758. [PubMed: 20592196]
25. Badea TC, Cahill H, Ecker J, Hattar S, Nathans J. Distinct Roles of Transcription Factors Brn3a and Brn3b in Controlling the Development, Morphology, and Function of Retinal Ganglion Cells. Neuron. 2009; 61:852–864. [PubMed: 19323995]
26. Ecker JL, et al. Melanopsin-Expressing Retinal Ganglion-Cell Photoreceptors: Cellular Diversity and Role in Pattern Vision. Neuron. 2010; 67:49–60. [PubMed: 20624591]
27. Godement P, Salaün J, Imbert M. Prenatal and postnatal development of retinogeniculate and retinocollicular projectionsin the mouse. The Journal of Comparative Neurology. 1984; 230:552–575. [PubMed: 6520251]
28. Xu, H-p, et al. An Instructive Role for Patterned Spontaneous Retinal Activity in Mouse Visual Map Development. Neuron. 2011; 70:1115–1127. [PubMed: 21689598]
29. Butts DA, Rokhsar DS. The Information Content of Spontaneous Retinal Waves. The Journal of Neuroscience. 2001; 21:961–973. [PubMed: 11157082]
30. Chandrasekaran AR, Plas DT, Gonzalez E, Crair MC. Evidence for an Instructive Role of Retinal Activity in Retinotopic Map Refinement in the Superior Colliculus of the Mouse. The Journal of Neuroscience. 2005; 25:6929–6938. [PubMed: 16033903]
31. Muir-Robinson G, Hwang BJ, Feller MB. Retinogeniculate Axons Undergo Eye-Specific Segregation in the Absence of Eye-Specific Layers. The Journal of Neuroscience. 2002; 22:5259–5264. [PubMed: 12097474]
32. Pfeiffenberger C, Yamada J, Feldheim DA. Ephrin-As and Patterned Retinal Activity Act Together in the Development of Topographic Maps in the Primary Visual System. The Journal of Neuroscience. 2006; 26:12873–12884. [PubMed: 17167078]
33. Torborg CL, Hansen KA, Feller MB. High frequency, synchronized bursting drives eye-specific segregation of retinogeniculate projections. Nat Neurosci. 2005; 8:72–78. [PubMed: 15608630]
34. Tritsch NX, Yi E, Gale JE, Glowatzki E, Bergles DE. The origin of spontaneous activity in the developing auditory system. Nature. 2007; 450:50–55. [PubMed: 17972875]
35. Garaschuk L, Linn J, Eilers J, Konnerth A. Large-scale oscillatory calcium waves in the immature cortex. Nat Neurosci. 2000; 3:452–459. [PubMed: 10769384]

36. Watt AJ, et al. Traveling waves in developing cerebellar cortex mediated by asymmetrical Purkinje cell connectivity. Nat Neurosci. 2009; 12:463–473. [PubMed: 19287389]
37. Kastanenka KV, Landmesser LT. In Vivo Activation of Channelrhodopsin-2 Reveals That Normal Patterns of Spontaneous Activity Are Required for Motoneuron Guidance and Maintenance of Guidance Molecules. The Journal of Neuroscience. 2010; 30:10575–10585. [PubMed: 20686000]
38. Vislay-Meltzer RL, Kampff AR, Engert F. Spatiotemporal Specificity of Neuronal Activity Directs the Modification of Receptive Fields in the Developing Retinotectal System. Neuron. 2006; 50:101–114. [PubMed: 16600859]
39. Demas JA, Payne H, Cline HT. Vision drives correlated activity without patterned spontaneous activity in developing Xenopus retina. Developmental Neurobiology. 201110.1002/dneu.20880
40. Kerschensteiner D, Wong ROL. A Precisely Timed Asynchronous Pattern of ON and OFF Retinal Ganglion Cell Activity during Propagation of Retinal Waves. Neuron. 2008; 58:851–858. [PubMed: 18579076]
41. Dan Y, Poo MM. Spike Timing-Dependent Plasticity: From Synapse to Perception. Physiological Reviews. 2006; 86:1033–1048. [PubMed: 16816145]
42. Weliky M, Katz LC. Disruption of orientation tuning visual cortex by artificially correlated neuronal activity. Nature. 1997; 386:680–685. [PubMed: 9109486]
43. Xu, H-p, et al. The Immune Protein CD3 Is Required for Normal Development of Neural Circuits in the Retina. Neuron. 2010; 65:503–515. [PubMed: 20188655]
44. Dhande OS, et al. Development of Single Retinofugal Axon Arbors in Normal and β2 Knock-Out Mice. The Journal of Neuroscience. 2011; 31:3384–3399. [PubMed: 21368050]
45. Huberman AD, et al. Architecture and Activity-Mediated Refinement of Axonal Projections from a Mosaic of Genetically Identified Retinal Ganglion Cells. Neuron. 2008; 59:425–438. [PubMed: 18701068]
46. Faguet J, Maranhao B, Smith SL, Trachtenberg JT. Ipsilateral Eye Cortical Maps Are Uniquely Sensitive to Binocular Plasticity. Journal of Neurophysiology. 2009; 101:855–861. [PubMed: 19052109]
47. Petros TJ, Rebsam A, Mason CA. Retinal axon growth at the optic chiasm: To cross or not to cross. Annual Review of Neuroscience. 2008; 31:295–315.
48. Crair MC, Gillespie DC, Stryker MP. The Role of Visual Experience in the Development of Columns in Cat Visual Cortex. Science. 1998; 279:566–570. [PubMed: 9438851]
49. Huberman AD, Speer CM, Chapman B. Spontaneous Retinal Activity Mediates Development of Ocular Dominance Columns and Binocular Receptive Fields in V1. Neuron. 2006; 52:247–254. [PubMed: 17046688]
50. Swindell EC, et al. Rx-Cre, a tool for inactivation of gene expression in the developing retina. genesis. 2006; 44:361–363. [PubMed: 16850473]

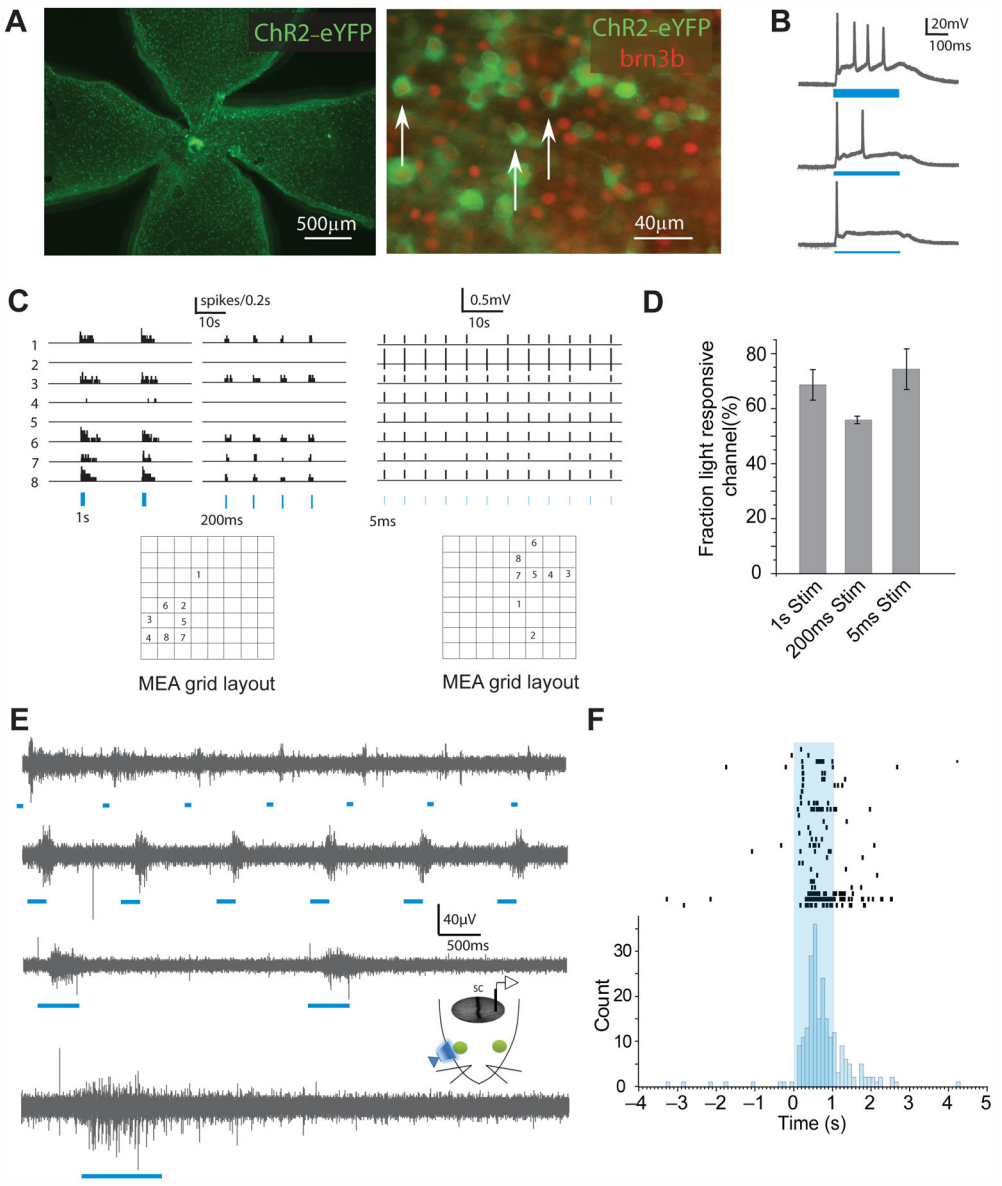

Figure 1. ChR2-expressing retinal ganglion cells (RGCs) are activated with high temporal precision with blue light both *in vitro* and *in vivo*

(A) Left panel: ChR2-expressing RGCs in *Thy1*-ChR2 transgenic mice are distributed across the entire retina; Right panel: Brn3b positive RGCs in red, ChR2-expressing cells in green. White arrows show examples of RGCs expressing both brn3b and ChR2. (B) Whole cell recording of a ChR2 RGC in response to 300 ms light stimuli at intensities of 0.65, 0.325 and 0.1625 mW/mm^2 (from top to bottom; mercury lamp filtered). Blue bars represent the presence of light stimuli; thickness represents the relative light intensity.(D) A few example channels from a multielectrode array (MEA) recording of whole mount retina in response to light stimuli (blue bars) of 1 s at 0.51 mW/mm^2 (left panel) and 5 ms at 3.18 mW/mm^2 (right panel). (E) –*In vivo* extracellular multiunit activity in superior colliculus neurons in response to 50 ms, 200 ms, 500 ms and 1s (top to bottom) light stimuli to the contralateral eye under 1% isoflurane anaesthesia. The light intensity is 0.64 mW/mm^2 immediately

outside the cornea. (F) Raster plot of *in vivo* responses to 1s light stimuli. Error bars represent s.e.m. Animals were between P9-P11.

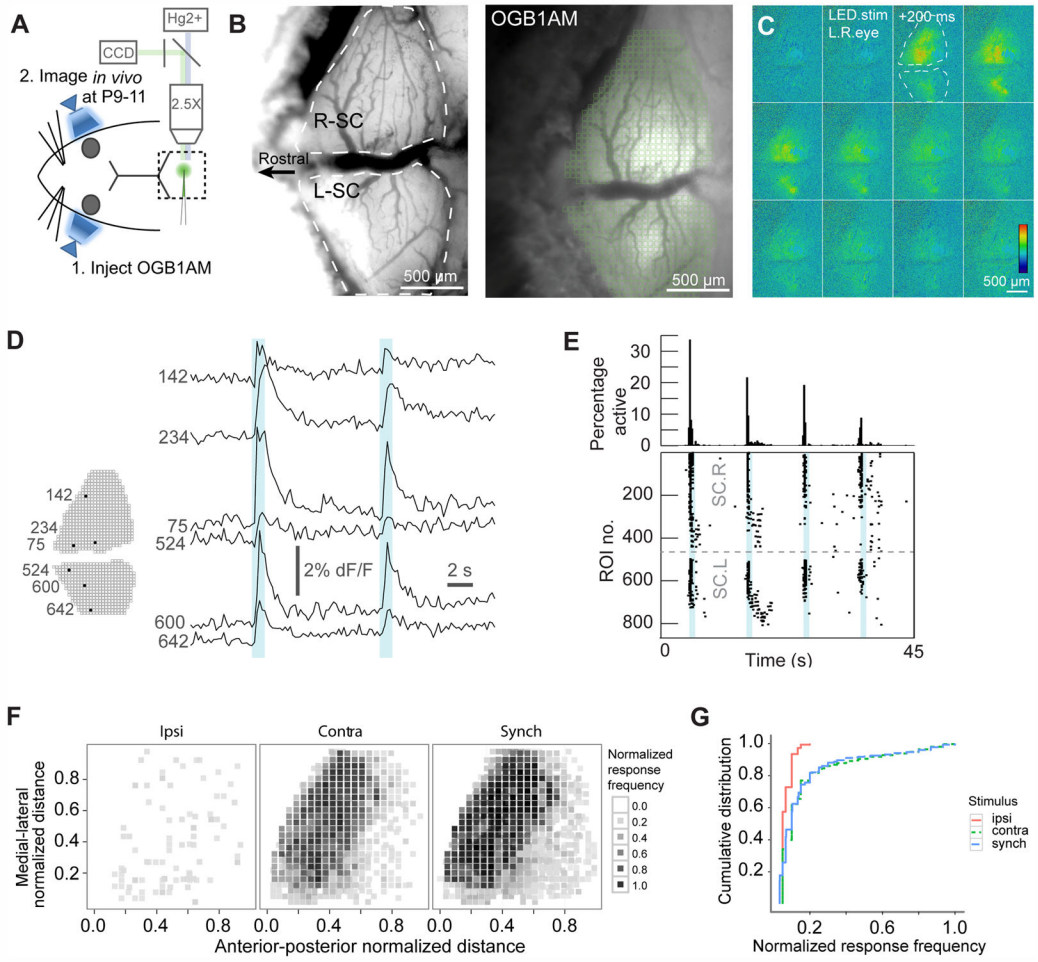

Figure 2. *In vivo* Ca^{2+} imaging demonstrates that a majority of superior colliculus neurons respond to optogentic stimuli before eye opening

(A) Experimental setup for *in vivo* calcium imaging. (B) Left panel is a bright field image of the craniotomy. White dashed line shows outlines for the right and left hemisphere of the superior colliculus (R-SC and L-SC, respectively). Right panel is the baseline OGB1AM fluorescent image. Each green square in the image is one region-of-interest (ROI). (C) Time lapse images of OGB1AM fluorescent signals in the superior colliculus due to synchronous LED stimulation of both eyes lasting 1 second starting at the second frame (200 ms interval between frames). Orientation of each frame is the same as in panel B. Color bar represents the normalized fluorescence change (ΔF/F from minimum to maximum). (D) Real-time calcium signals (raw traces) for individual ROIs (indicated by numbers) show that synchronous optogenetic stimulation of both eyes drives synchronous neuronal response in the superior colliculus of both hemispheres. One second long light stimuli occurred at the times indicated by blue shading. (E) Real-time raster plots for responses from all ROIs and the fraction of active ROIs to four consecutive light stimuli that occurred at the time of blue shading. (F) Normalized response frequency for each ROI in one hemisphere of the superior colliculus to stimulation of the ipsilateral (ipsi), contralateral (contra) or both eyes (synch) (n = 3 experiments for ipsi and contra, n = 5 experiments for synch). (G) Cumulative distribution of normalized response frequency for ipsi, contra and synch in (F). There is little

response to stimulation of the ipsilateral eye itself, but strong response to stimulation of the contralateral eye or synchronous stimulation of both eyes.

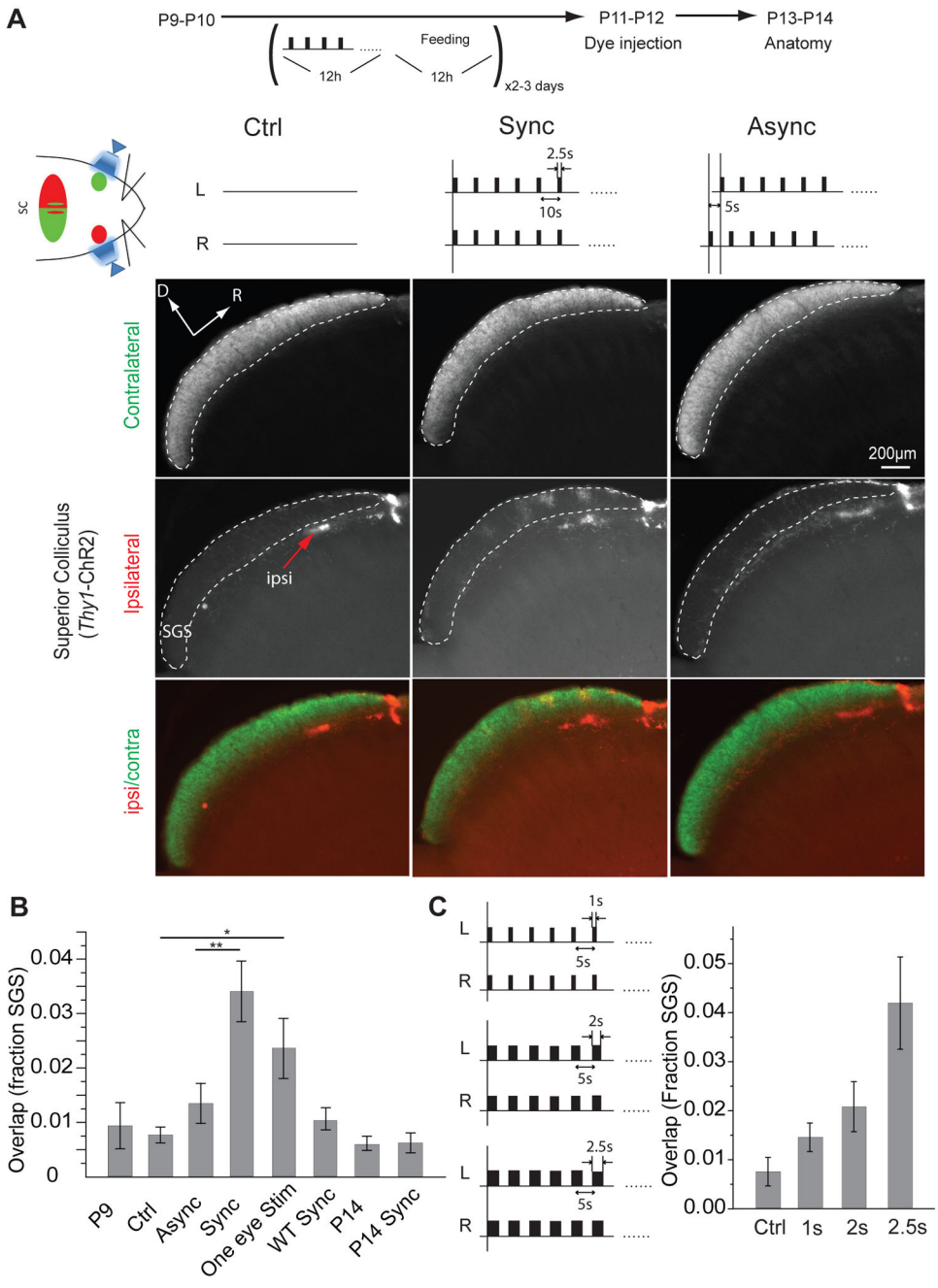

Figure 3. Synchronous but not asynchronous stimulation of both eyes disrupts eye-specific segregation in the superior colliculus

(A) Both eyes of *Thy1*-ChR2 mice were stimulated on a 12h stimulation - 12h feeding cycle for two-three days starting at P9. Panels show parasagittal sections through the superior colliculus. Ipsilateral axons (red arrow) normally terminate in clusters in the rostral superior colliculus just inferior to the contralateral layer (SGS, dotted line). Synchronous stimulation (middle column) caused axons from the ipsilateral eye (grey scale signal) to form abnormal clusters in the contralateral (SGS) layer; asynchronous stimulation (right column) didn't affect eye segregation in comparison to unstimulated controls (left column). (B)

Quantification of stimulation and control experiments by measuring the fraction of the contralateral (SGS) layer which is occupied by ipsilateral pixels. P9 (n = 3) and P14 (n = 4) results from unmanipulated *Thy1*-ChR2 mice; Ctrl (n = 5) is *Thy1*-ChR2 mice which were manipulated daily the same as experimental mice, but were not optically stimulated; Async (n = 8) and Sync (n = 6) were asynchronously and synchronously stimulated *Thy1*-ChR2 mice; One eye Stim (n = 2) were *Thy1*-ChR2 mice with the ipsilateral eye only stimulated; WT Sync: synchronously stimulated wild-type mice lacking ChR2 (n = 5); P14 Sync (n = 3): synchronously stimulated *Thy1*-ChR2 mice starting at P14. (C) Results from experiments in which stimuli with the same frequency (0.2 Hz or 5 sec between stimuli) but varying durations (1 s, n = 4; 2 s, n = 3; 2.5 s, n = 5) show that eye segregation got worse as the duration of synchronous activity increased. * $p < 0.05$, ** $p < 0.005$. Error bars represent s.e.m.. R: rostral; D: Dorsal. L: Left eye; R: Right eye.

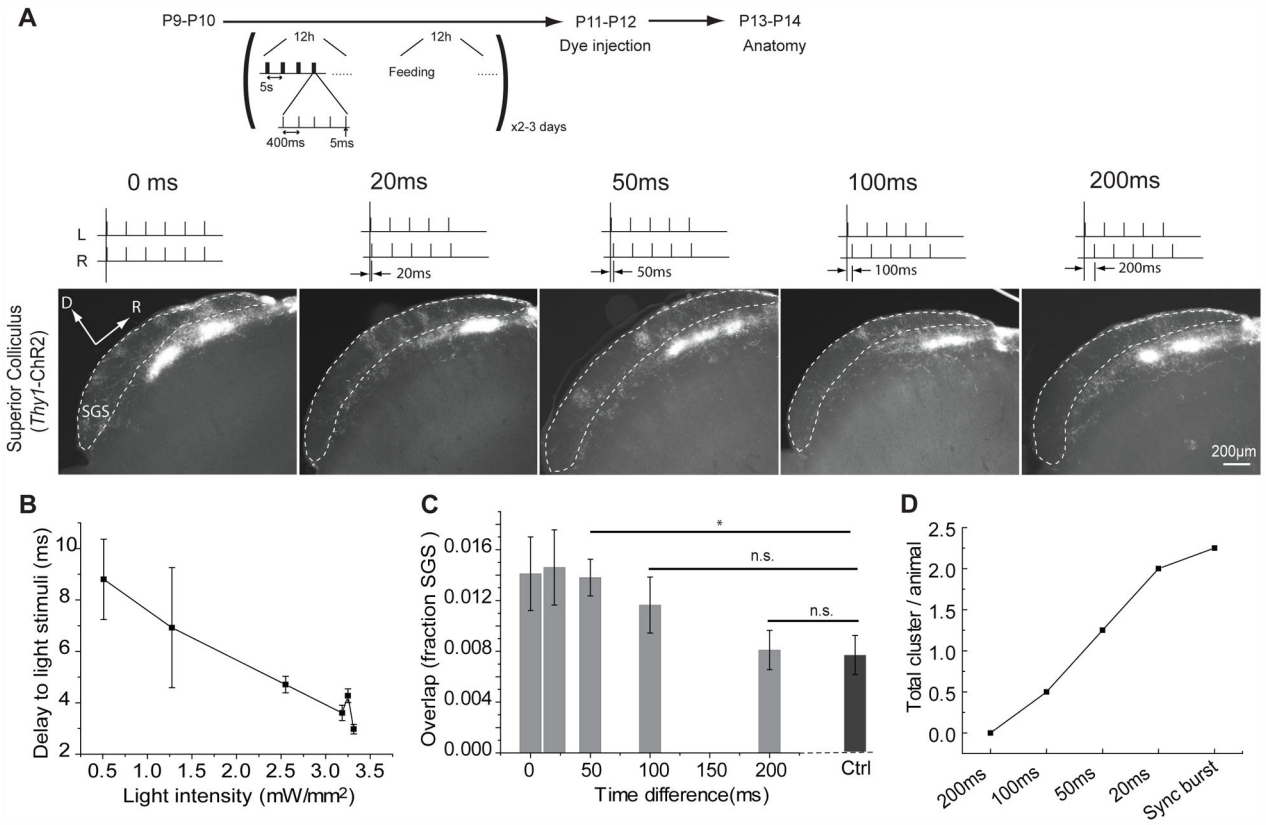

Figure 4. As much as 100 msec asynchronous binocular stimulation disturbs eye segregation

(A) Bursts of 5 msec light pulses were used to stimulate both eyes in *Thy1*-ChR2 mice with a timing difference of 0 s (n = 4), 20 ms (n = 3), 50 ms (n = 4), 100 ms (n = 4) and 200 ms (n = 5) between the two eyes. (B) The delay of RGC spiking responses to the onset of the 5 ms light stimuli with a range of different light intensities *in vitro* is less than 10 ms, and not very variable, particularly at higher light intensities. Error bars represent S.D.. (C) Eye segregation in the superior colliculus was not disturbed with asynchronous stimuli with a 200 ms difference between the eyes, but got worse as the temporal difference between the two eyes decreased. (D) The total number of ipsilateral clusters in the contralateral SGS layer per animal increased as the optogenetic stimulation became increasingly synchronous. n.s., not significant ($p > 0.05$); * $p < 0.05$, ** $p < 0.005$. Error bars represent s.e.m..

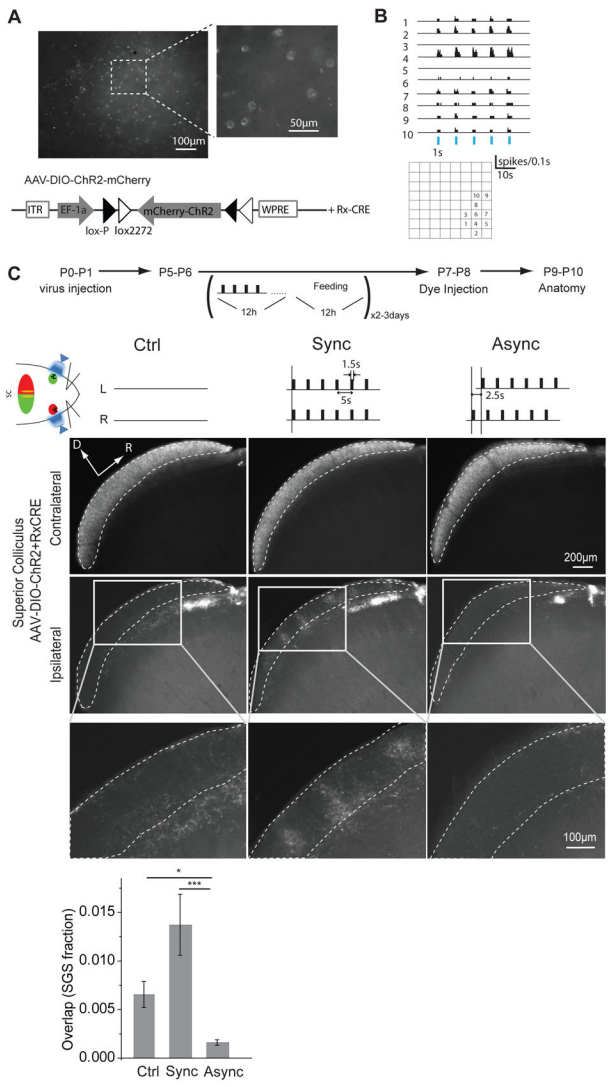

Figure 5. Synchronous stimulation disrupted eye segregation and asynchronous stimulation improved eye segregation during development in AAV-ChR2 treated mice

(A) Injection of AAV-DIO-ChR2-mCherry virus into retinas of P0-P1 Rx-Cre mice induced the expression of ChR2 in RGCs 5 days later. Viral exposure induced ChR2 expression in neurons that express CRE. Example shows ChR2 expression in RGCs in the ventral-temporal retina (binocular zone) of Rx-CRE mice 5 days after intravitreous injection of the AAV-DIO-ChR2-mCherry virus. (B) Example Multielectrode Array (MEA) recording from a whole mount retina in response to 1s light stimuli of 2.55 mW/mm^2 in these mice. Blue bars represent the light stimuli. (C) Synchronous stimulation of both eyes (Sync, n = 4) when eye-specific segregation is just emerging (P5-P6) disturbed segregation in the superior colliculus, whereas asynchronous stimulation (Async, n = 6) improved segregation in comparison to control animals (Ctrl, n = 4). Gray boxes in the upper images indicated the area in the high–magnification images below. * $p < 0.05$, *** $p < 0.001$. Error bars represent s.e.m..

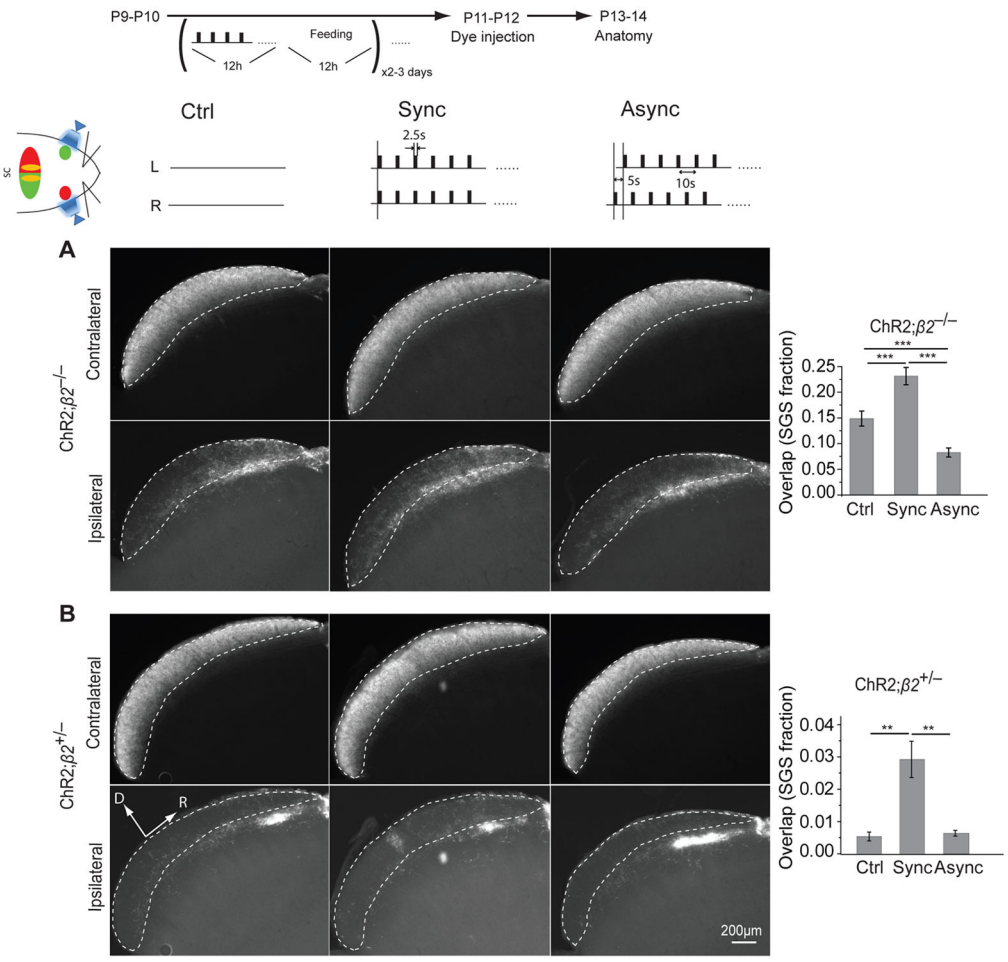

Figure 6. Synchronous stimulation disrupted and asynchronous stimulation improved eye-specific segregation in ChR2;$\beta2^{-/-}$ mice

(A) Eye segregation for synchronously stimulated ChR2;$\beta2^{-/-}$ mice (Sync, n = 5) is worse than in $\beta2^{-/-}$ controls (Ctrl, n = 4). Asynchronous stimulation in ChR2;$\beta2^{-/-}$ (Async, n = 3) substantially improved eye segregation in comparison to $\beta2^{-/-}$ controls. (B) As expected, synchronous (Sync, n = 6) and asynchronous (Async, n = 4) light stimulation had a similar effect in ChR2;$\beta2^{+/-}$ mice as in *Thy1*-ChR2 mice (Figure 3B) (ChR2;$\beta2^{+/-}$ control, n = 3). n.s., not significant ($p > 0.05$), ** $p < 0.005$, *** $p < 0.001$. Error bars represent s.e.m..

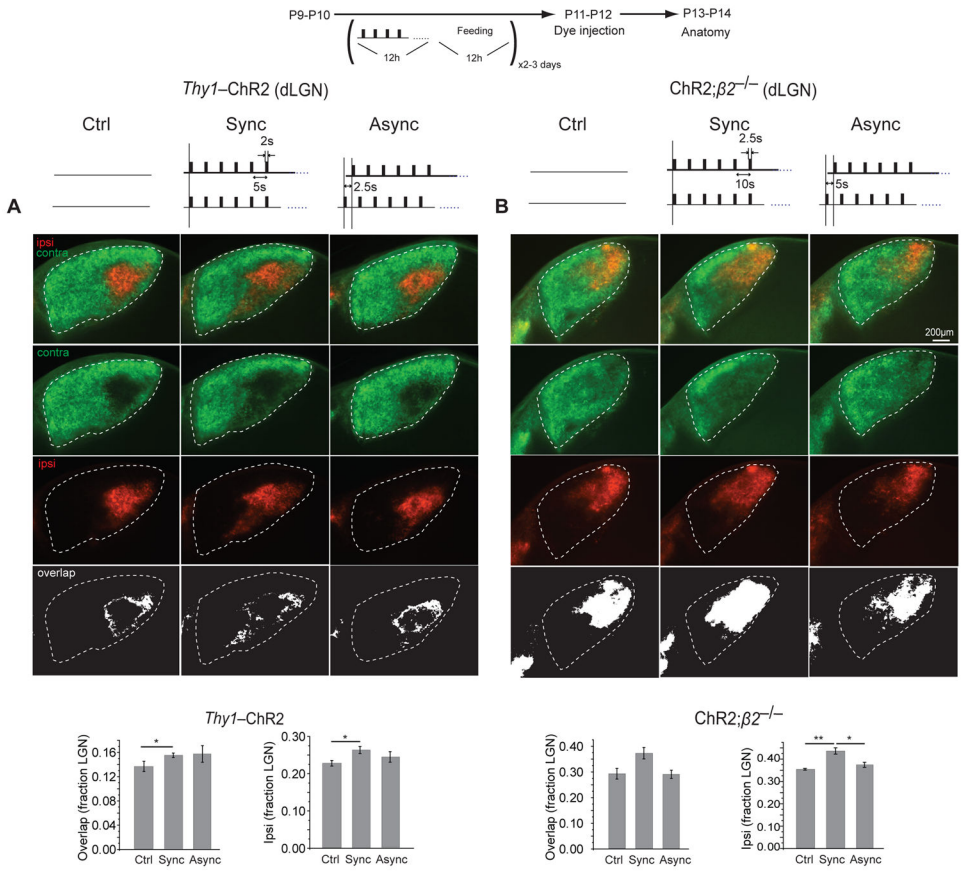

Figure 7. Synchronous stimulation disrupts eye segregation in the dLGN

Synchronous stimulation caused an increase in the overlap (white – bottom row) between ipsilateral (red) and contralateral (green) axons in both (A) *Thy1*-ChR2 and (B) ChR2;$\beta2^{-/-}$ mice. Asynchronous stimulation didn't affect eye segregation. n = 5 for *Thy1*-ChR2 Ctrl, n = 3 for *Thy1*-ChR2 Syn, n = 4 for *Thy1*-ChR2 Async; n = 4 for ChR2;$\beta2^{-/-}$ Ctrl, n = 3 for ChR2;$\beta2^{-/-}$ Syn, n = 4 for ChR2;$\beta2^{-/-}$ Async. * $p < 0.05$, ** $p < 0.005$. Error bars represent s.e.m..

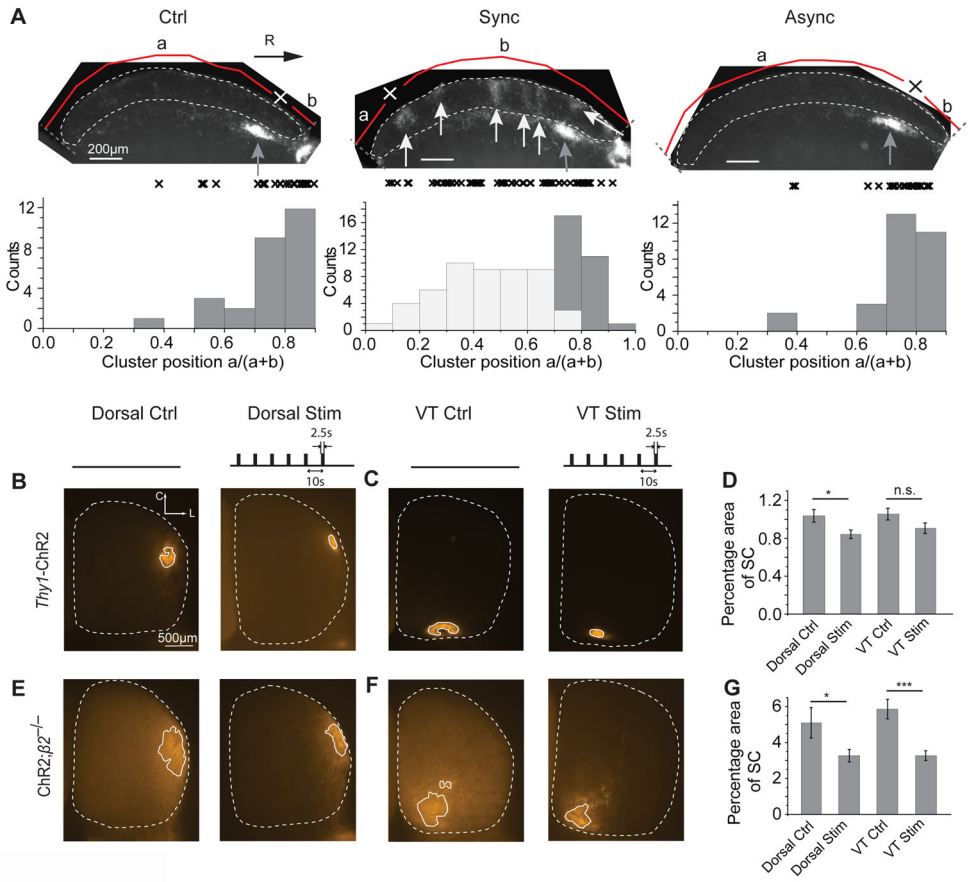

Figure 8. Chronic stimulation of ChR2-expressing RGCs disrupts retinotopy of ipsilateral RGCs, but improves retinotopy of contralateral RGCs

(A) Distribution of ipsilateral axon arbor clusters along the rostral-caudal axis of the superior colliculus in *Thy1*-ChR2 experiments. The ipsilateral domains of both control (Ctrl, n = 28 sections) and asynchronously stimulated animals (Async, same as Figure 3, n = 28 sections) are located only in the rostral superior colliculus just inferior to the SGS layer (dark grey arrows and histogram). Ipsilateral clusters in the SGS caused by synchronous stimulation are distributed throughout the rostral-caudal axis of the superior colliculus (Sync, n = 52 sections, light grey arrows and histogram). Normal ipsilateral domains in the SO layer just inferior to the SGS are located similarly in the control, synchronous and asynchronously stimulated mice (Sync, n = 24 sections, dark grey arrows and histogram). Each “x” represents the relative position of one cluster, which is calculated by the distance to the caudal end of the SGS (a) divided by the total length from the caudal to the rostral end of the SGS (a+b). Light and dark grey arrows indicate the ipsilateral clusters in the SGS (light grey) and the SO layer just inferior to the SGS (dark grey) where ipsilateral axons normally terminate. (B, C) Whole mount superior colliculus images (dorsal view; outlined by white dotted line) of control (Ctrl) and whole-eye stimulated (Stim) *Thy1*-ChR2 mice with focal injections of DiI into the dorsal or ventral-temporal (VT) retinas. (D) Chronic optogenetic stimulation resulted in smaller target zones in the superior colliculus for dorsal projections (Dorsal, n = 22, $p < 0.05$) and a similar trend for ventral-temporal projections (VT; n = 17) in comparison to Ctrl mice (Dorsal Ctrl, n = 8; VT Ctrl, n = 14) in *Thy1*-ChR2

animals. (E, F) Whole mount superior colliculus images of control (Ctrl) and whole-eye stimulated (Stim) ChR2;$\beta2^{-/-}$ mice with focal injections of DiI into the dorsal or ventral-temporal retinas. (G) Similar to *Thy1*-ChR2 mice, ChR2;$\beta2^{-/-}$ mice also had smaller target zones in the superior colliculus for both dorsal (Dorsal, $n = 11$, $p < 0.05$) and ventral-temporal (VT, $n = 12$, $p < 0.001$) projections after chronic optical stimulation (Dorsal Ctrl $n = 5$, VT Ctrl $n = 5$). n.s., not significant ($p > 0.05$); * $p < 0.05$, *** $p < 0.001$. Error bars represent s.e.m.. C is caudal, L is lateral.